Supplementary Figures

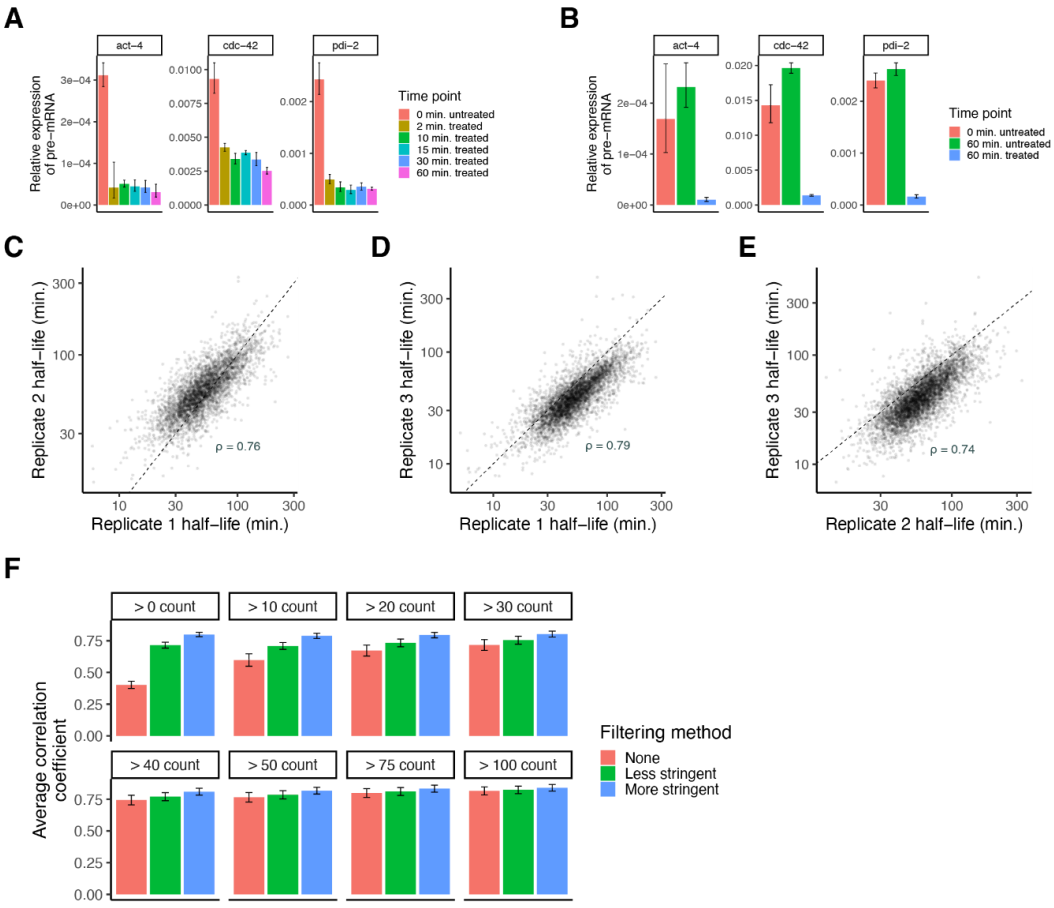

Supplemental Figure S1. Quality control for transcription inhibition approach paired with bulk RNA-sequencing. (A) Bar plots showing the relative expression of pre-mRNA for the housekeeping genes *act-4*, *cdc-42*, and *pdi-2* in embryonic cells following different lengths of transcription inhibition with actD. Expression was measured using RT-qPCR (quantitative reverse transcription PCR). Error bars represent variation in expression across three technical replicates. (B) Bar plots showing the relative expression of pre-mRNA for the housekeeping genes *act-4*, *cdc-42*, and *pdi-2* in embryonic cells following no treatment of actD, 60 minutes of treatment with actD, and 60 minutes with no treatment of actD. Expression was measured using RT-qPCR. Error bars represent variation in expression across three technical replicates. (C, D, E) Scatter plots showing the comparison of measured mRNA half-lives between three biological replicates on a log-log scale. Genes were compared if they had count > 30 at the 0 minute time point and if their decay fit an exponential decay model $R^2 \geq 0.75$ for each replicate. Spearman correlation coefficient is displayed for each pairwise comparison. Dashed line is the x = y line. (F) Bar plot showing the average Pearson correlation coefficient between mRNA half-lives across pairwise comparisons of three biological replicates under different count thresholds at the 0 minute time point and filtering methods. The less stringent filtering method only included genes if their coefficient of variation (standard deviation/mean*100) across biological replicates was ≤ 50% or the fold-change between the upper limit of their 95% confidence interval and measured half-life was ≤ 3. The stringent filtering method only included genes if their coefficient of variation across biological replicates was ≤ 30% or the fold-change between the upper limit of their 95% confidence interval and measured half-life was ≤ 2. Error bars represent standard deviation of the Pearson correlation coefficient among the three biological replicates.

A

Term	Expected	Observed	Enrichment.Fold.Change	P.value	Q.value
cytosolic large ribosomal subunit GO:0022625	3.8	25	6.5	0.0e+00	0.0e+00
extracellular region GO:0005576	21.0	62	2.9	7.2e−17	1.0e−14
structural constituent of ribosome GO:0003735	14.0	47	3.4	1.3e−16	1.2e−14
proton transmembrane transport GO:1902600	7.5	30	4.0	3.6e−14	2.5e−12
supramolecular polymer GO:0099081	37.0	79	2.1	6.6e−12	3.7e−10
calcium ion binding GO:0005509	15.0	41	2.8	3.0e−11	1.4e−09
muscle system process GO:0003012	7.2	26	3.6	4.1e−11	1.7e−09
structural constituent of chromatin GO:0030527	5.1	21	4.1	4.1e−11	1.7e−09
transmembrane transport GO:0055085	58.0	105	1.8	1.2e−10	3.6e−09
structural constituent of cytoskeleton GO:0005200	3.4	16	4.7	1.7e−10	4.9e−09
myofibril GO:0030016	13.0	37	2.8	1.8e−10	4.9e−09
actin binding GO:0003779	15.0	40	2.6	5.8e−10	1.4e−08
transporter activity GO:0005215	57.0	102	1.8	6.3e−10	1.4e−08
external encapsulating structure GO:0030312	7.1	24	3.4	1.1e−09	2.2e−08
purine nucleoside triphosphate metabolic process GO:0009144	4.5	17	3.8	1.4e−08	2.6e−07
protein heterodimerization activity GO:0046982	6.8	21	3.1	7.9e−08	1.4e−06
peptide biosynthetic process GO:0043043	39.0	71	1.8	1.5e−07	2.5e−06
muscle cell development GO:0055001	6.3	19	3.0	5.1e−07	8.1e−06
actin filament−based process GO:0030029	26.0	50	1.9	1.0e−06	1.5e−05
A band GO:0031672	5.2	16	3.1	2.4e−06	3.4e−05

B

Term	Expected	Observed	Enrichment.Fold.Change	P.value	Q.value
DNA−binding transcription factor activity GO:0003700	36.0	75	2.1	5.6e−11	1.6e−08
sequence−specific DNA binding GO:0043565	43.0	85	2.0	7.7e−11	1.6e−08
RNA biosynthetic process GO:0032774	85.0	140	1.6	6.4e−10	6.1e−08
cellular aromatic compound metabolic process GO:0006725	200.0	275	1.4	1.0e−09	7.1e−08
heterocycle metabolic process GO:0046483	200.0	274	1.4	1.4e−09	8.2e−08
organic cyclic compound metabolic process GO:1901360	200.0	275	1.4	3.5e−09	1.7e−07
transcription regulatory region nucleic acid binding GO:0001067	31.0	61	1.9	7.3e−08	3.0e−06
double−stranded DNA binding GO:0003690	36.0	67	1.9	8.9e−08	3.2e−06
condensed chromosome centromeric region GO:0000779	7.8	22	2.8	6.4e−07	2.0e−05
formation of primary germ layer GO:0001704	3.3	11	3.3	2.4e−05	6.8e−04
recombinational repair GO:0000725	5.1	14	2.8	5.3e−05	1.4e−03
metabolic process GO:0008152	410.0	475	1.2	1.2e−04	2.9e−03
protein−DNA complex GO:0032993	51.0	74	1.5	3.1e−04	6.8e−03
single−stranded DNA binding GO:0003697	3.8	10	2.6	7.2e−04	1.5e−02
nucleic acid transport GO:0050657	6.9	15	2.2	7.4e−04	1.5e−02
mRNA transport GO:0051028	5.1	12	2.4	8.5e−04	1.5e−02
meiotic cell cycle GO:0051321	20.0	33	1.7	1.1e−03	1.8e−02
RNA localization GO:0006403	7.1	15	2.1	1.2e−03	1.9e−02
cell−cell signaling by wnt GO:0198738	5.5	12	2.2	1.9e−03	2.9e−02
import into nucleus GO:0051170	5.2	11	2.1	3.7e−03	5.3e−02

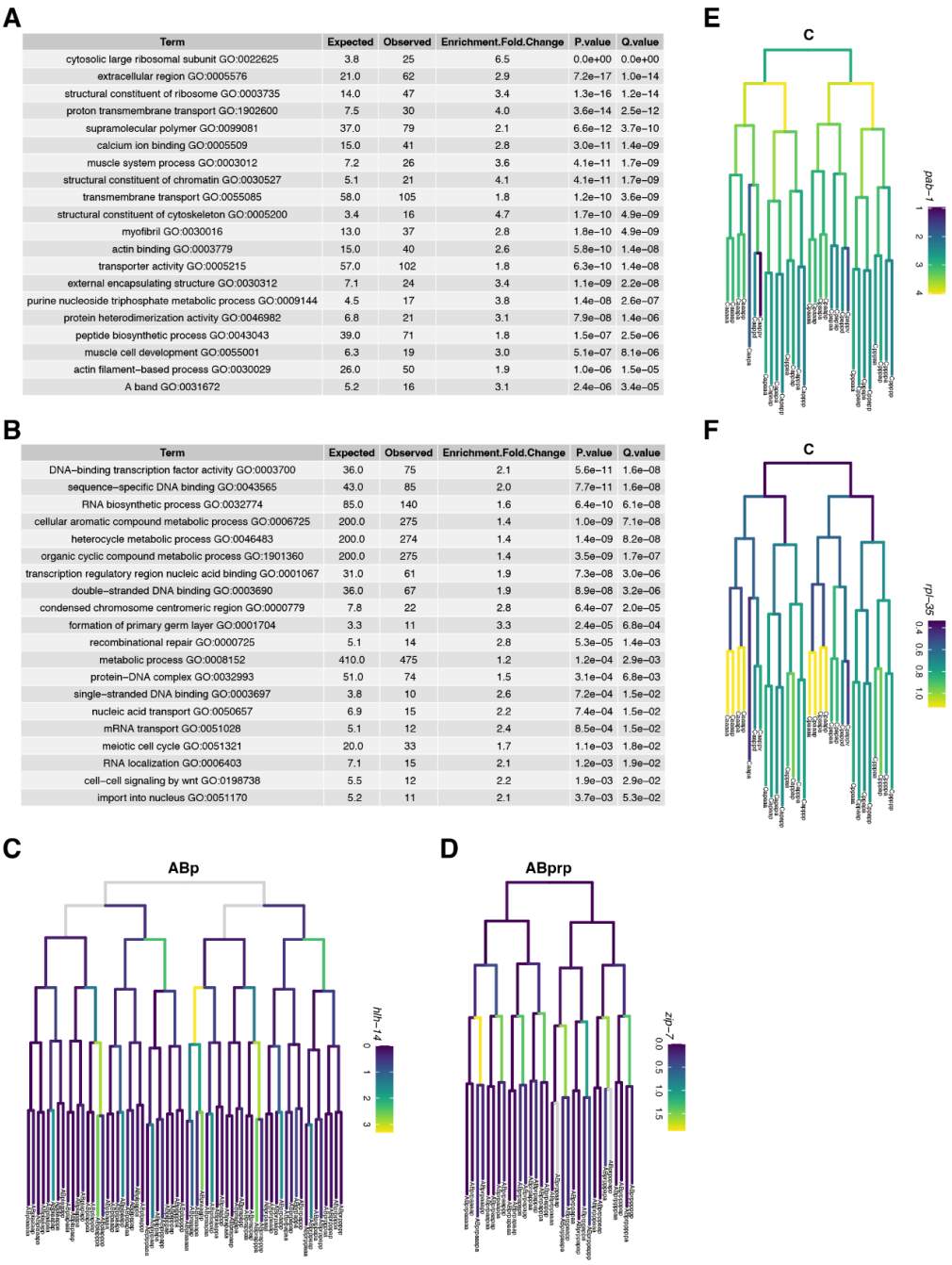

Supplemental Figure S2. Extended gene ontology analysis results for bulk data and lineage tree examples of highly transient and persistent genes. (A) Twenty most significantly enriched gene ontology terms for the top 15% stable transcripts. Background set of genes used was all genes that met our moderate mRNA half-life filtering metric. (B) Twenty most significantly enriched gene ontology terms for the top 15% unstable transcripts. Background set of genes used was all genes that met our moderate mRNA half-life filtering metric. (C, D, E, F) Sublineages with coloring representing gene expression from our *C. elegans* embryo single cell atlas (Packer et al. 2019).

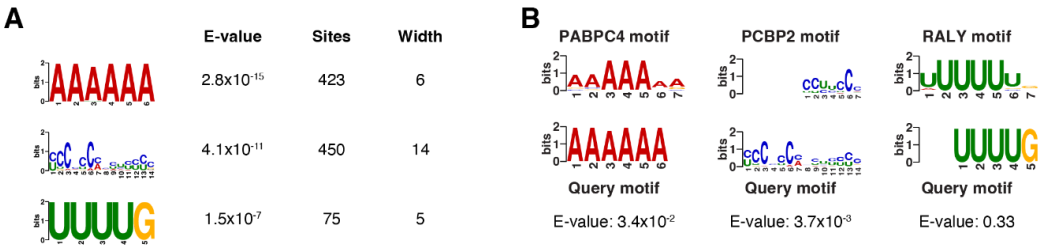

Supplemental Figure S3. Extended motif analysis results for stable transcripts in the bulk data. (A) Motifs found to be differentially enriched in the 3' UTRs of the top 15% stable transcripts using the *de novo* motif-finding program MEME (Bailey et al. 2015), including the E-value, number of sites found, and width for each motif. The 3' UTRs of the top 15% unstable transcripts were used as control sequences. (B) Mammalian motifs with the highest similarity to the motifs identified in (A) using the Tomtom motif comparison tool against a database of known motifs (Ray et al. 2013).

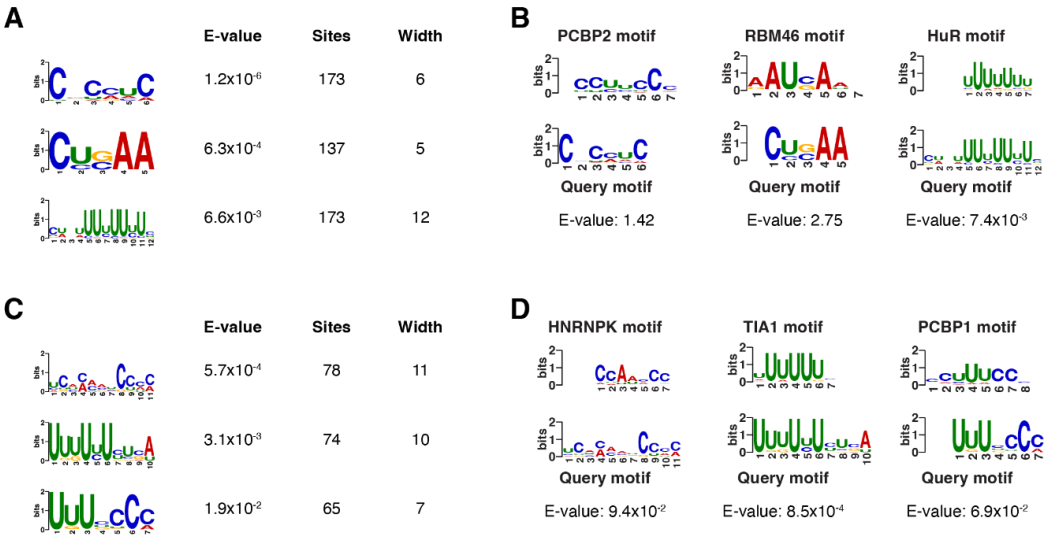

Supplemental Figure S4. Extended motif analysis results for genes that accumulate to high transcript levels. (A) Motifs found to be differentially enriched in the 3' UTRs of genes that accumulate to high transcript levels ~200 minutes past the four-cell stage in a whole embryo RNA-seq dataset (Hashimshony et al. 2015). Motifs were identified using the *de novo* motif-finding program MEME (Bailey et al. 2015). Table includes the E-value, number of sites found, and width for each motif. The 3' UTRs of genes that accumulate to low transcript levels ~200 minutes were used as control sequences. (B) Mammalian motifs with the highest similarity to the motifs identified in (A) using the Tomtom motif comparison tool against a database of known motifs (Ray et al. 2013). (C) Motifs found to be differentially enriched in the 3' UTRs of genes that accumulate to high transcript levels ~350 minutes past the four-cell stage in a whole embryo RNA-seq dataset (Hashimshony et al. 2015). Motifs were identified using the *de novo* motif-finding program MEME (Bailey et al. 2015). Table includes the E-value, number of sites found, and width for each motif. The 3' UTRs of genes that accumulate to low transcript levels ~350 minutes were used as control sequences. (D) Mammalian motifs with the highest similarity to the motifs identified in (C) using the Tomtom motif comparison tool against a database of known motifs (Ray et al. 2013).

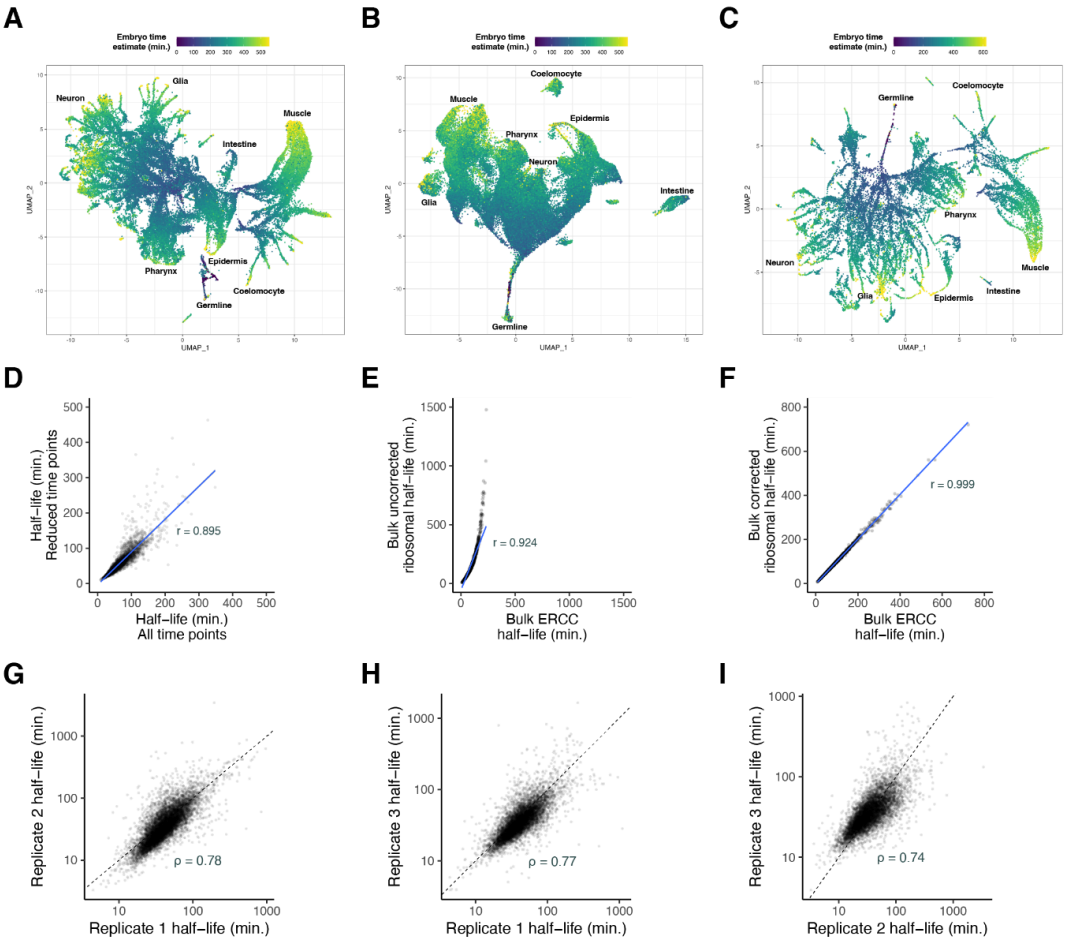

Supplemental Figure S5. Quality control for transcription inhibition approach paired with single-cell RNA-sequencing. (A, B, C) Global UMAPs for individual biological replicates, with cells colored by embryo age as estimated from correlations to a whole-embryo RNA-sequencing time series (Hashimshony et al. 2015). Trajectories corresponding to major cell types are labeled. (D) Scatter plot showing the comparison of calculated mRNA half-lives when using all time points (0, 10, 20, 40, 60 minutes) or reduced time points (0, 20, 40 minutes) from the bulk data. Genes were compared if they met the following criteria: coefficient of variation across biological replicates ≤ 50% or the fold-change between the upper limit of their 95% confidence interval and measured half-life ≤ 3. To better include high-stability mRNAs, genes with half-lives > 100 minutes were allowed a looser filtering strategy. Such genes were included if their half-lives had a coefficient of variation ≤ 75% or fold-change between the upper limit of their 95% confidence interval and measured half-life ≤ 4. Pearson's correlation coefficient = 0.895. (E) Scatter plot showing the comparison in calculated mRNA half-lives from the bulk data between gene counts normalized to spike-in ERCC transcripts or transcripts encoding ribosomal proteins. Pearson's correlation coefficient = 0.924. Blue line is the best fit line. (F) Scatter plot showing the comparison in calculated mRNA half-lives from the bulk data between gene counts normalized to spike-in ERCC transcripts or transcripts encoding ribosomal proteins after correcting for their decay. Pearson's correlation coefficient = 0.999. Blue line is the best fit line. (G, H, I) Scatter plots showing the comparison of measured mRNA half-lives between 3 single-cell biological replicates on a log-log scale. Genes were compared if they had UMI > 30 at the 0 minute time point and if their decay fit an exponential decay model $R^2 \geq 0.75$ for each replicate. Spearman correlation coefficient is displayed for each pairwise comparison. Dashed line is the x = y line.

A

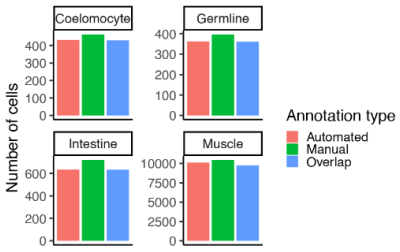

B

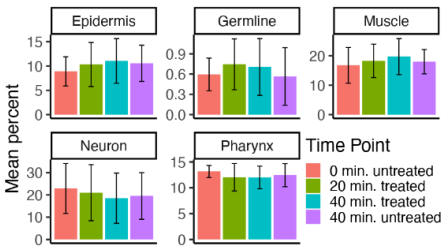

C

Group1	Group2	n1	n2	p	p.adjusted
Muscle	Germline	4350	802	2.21e−99	1.77e−98
Muscle	Epidermis	4350	3717	9.58e−06	1.92e−05
Muscle	Neuron	4350	4762	7.68e−30	3.84e−29
Muscle	Pharynx	4350	4700	7.00e−03	7.00e−03
Germline	Epidermis	802	3717	2.72e−75	1.90e−74
Germline	Neuron	802	4762	1.36e−186	1.36e−185
Germline	Pharynx	802	4700	1.78e−118	1.60e−117
Epidermis	Neuron	3717	4762	2.02e−55	1.21e−54
Epidermis	Pharynx	3717	4700	6.63e−13	1.99e−12
Neuron	Pharynx	4762	4700	1.00e−18	4.00e−18

Supplemental Figure S6. Quality control for transcription inhibition approach paired with single-cell RNA-sequencing continued. (A) Bar plot comparing the number of cells from the first biological replicate annotated as coelomocyte, germline, intestine, or muscle based on manual annotation using marker genes or automated annotation using Seurat. (B) Bar plot showing the mean percentage of cells coming from the epidermis, germline, muscle, neuron, and pharynx within each biological replicate, separated by time point. Error bars represent standard deviation between the three biological replicates. (C) Table comparing the mRNA half-life distributions between epidermis, germline, muscle, neuron, and pharynx and whether the distributions are statistically significant from one another. P-values comparing median half-lives were calculated using the Wilcoxon rank sum test.

A

Term	Expected	Observed	Enrichment.Fold.Change	P.value	Q.value
structural constituent of chromatin GO:0030527	1.50	10	6.7	1.2e−07	3.5e−05
protein heterodimerization activity GO:0046982	2.20	10	4.6	6.9e−06	9.8e−04
transmembrane transport GO:0055085	9.10	20	2.2	3.3e−04	3.2e−02
passive transmembrane transporter activity GO:0022803	1.80	7	3.8	3.9e−04	3.2e−02
symporter activity GO:0015293	0.42	3	7.1	5.0e−04	3.2e−02
transporter activity GO:0005215	8.80	19	2.2	5.7e−04	3.2e−02

B

Term	Expected	Observed	Enrichment.Fold.Change	P.value	Q.value
cilium organization GO:0044782	2.400	19	8.1	2.5e−14	7.1e−12
non−motile cilium assembly GO:1905515	1.100	12	11.0	6.4e−12	9.1e−10
ciliary basal body GO:0036064	1.100	9	8.4	2.9e−08	2.7e−06
cell projection GO:0042995	12.000	31	2.6	5.0e−07	3.6e−05
cell projection organization GO:0030030	10.000	27	2.6	1.4e−06	8.0e−05
microtubule−based transport GO:0099111	1.800	9	5.0	8.0e−06	3.8e−04
non−motile cilium GO:0097730	1.200	7	6.0	1.2e−05	4.8e−04
ciliary plasm GO:0097014	0.690	5	7.3	2.9e−05	1.0e−03
taxis GO:0042330	5.500	15	2.7	1.3e−04	4.0e−03
supramolecular polymer GO:0099081	8.100	18	2.2	5.2e−04	1.5e−02
monoatomic ion homeostasis GO:0050801	2.400	8	3.3	5.5e−04	1.5e−02
inorganic ion import across plasma membrane GO:0099587	0.490	3	6.1	9.5e−04	2.2e−02
neurotransmitter receptor activity involved in regulation of postsynaptic membrane potential GO:0099529	0.098	1	10.0	2.4e−03	5.2e−02
transmembrane transport GO:0055085	10.000	19	1.9	3.4e−03	6.9e−02
synaptic signaling GO:0099536	3.700	9	2.4	3.9e−03	7.3e−02
sodium ion transport GO:0006814	0.730	3	4.1	5.1e−03	9.0e−02
passive transmembrane transporter activity GO:0022803	2.700	7	2.6	5.1e−03	9.0e−02
gated channel activity GO:0022836	1.200	4	3.4	5.5e−03	9.0e−02
monocarboxylic acid biosynthetic process GO:0072330	0.780	3	3.8	6.5e−03	9.7e−02
chemosensory behavior GO:0007635	1.200	4	3.3	6.5e−03	9.7e−02

C

Term	Expected	Observed	Enrichment.Fold.Change	P.value	Q.value
structural constituent of chromatin GO:0030527	0.59	4	6.8	0.00016	0.045
transmembrane transport GO:0055085	8.00	18	2.3	0.00039	0.055
peptidase inhibitor activity GO:0030414	0.43	3	7.0	0.00049	0.055
endopeptidase regulator activity GO:0061135	0.43	3	7.0	0.00049	0.055
extrinsic component of cytoplasmic side of plasma membrane GO:0031234	0.48	3	6.2	0.00085	0.055
extracellular region GO:0005576	1.60	6	3.7	0.00088	0.055
proteoglycan metabolic process GO:0006029	0.54	3	5.6	0.00140	0.055
inorganic ion import across plasma membrane GO:0099587	0.27	2	7.4	0.00140	0.055
protein serine kinase activity GO:0106310	3.40	9	2.6	0.00210	0.066
potassium ion transmembrane transport GO:0071805	0.32	2	6.2	0.00280	0.078
chloride channel complex GO:0034707	0.11	1	9.3	0.00290	0.078
monoatomic anion transport GO:0006820	0.65	3	4.6	0.00290	0.078
monoatomic ion homeostasis GO:0050801	2.00	6	2.9	0.00380	0.082
cytosolic large ribosomal subunit GO:0022625	0.70	3	4.3	0.00400	0.082
endoplasmic reticulum subcompartment GO:0098827	7.00	14	2.0	0.00430	0.082
transporter activity GO:0005215	7.70	15	1.9	0.00450	0.082
symporter activity GO:0015293	0.38	2	5.3	0.00460	0.082
sodium ion transport GO:0006814	0.38	2	5.3	0.00460	0.082
nuclear outer membrane−endoplasmic reticulum membrane network GO:0042175	7.30	14	1.9	0.00620	0.092

Supplemental Figure S7. Extended gene ontology analysis results for genes with more rapid mRNA decay over time. (A) Significantly enriched gene ontology terms for the top 5% of genes with faster decay in Middle-stage cells compared to Early-stage cells. Background set of genes used was shared genes between Early- and Middle-stage cells that met our moderate mRNA half-life filtering metric. (B) Twenty most significantly enriched gene ontology terms for the top 5% of genes with faster decay in Late-stage cells compared to Middle-stage cells. Background set of genes used was shared genes between Middle- and Late-stage cells that met our moderate mRNA half-life filtering metric. (C) Significantly enriched gene ontology terms for the top 5% of genes with faster decay in Late-stage cells compared to Early-stage cells. Background set of genes used was shared genes between Early- and Late-stage cells that met our moderate mRNA half-life filtering metric.

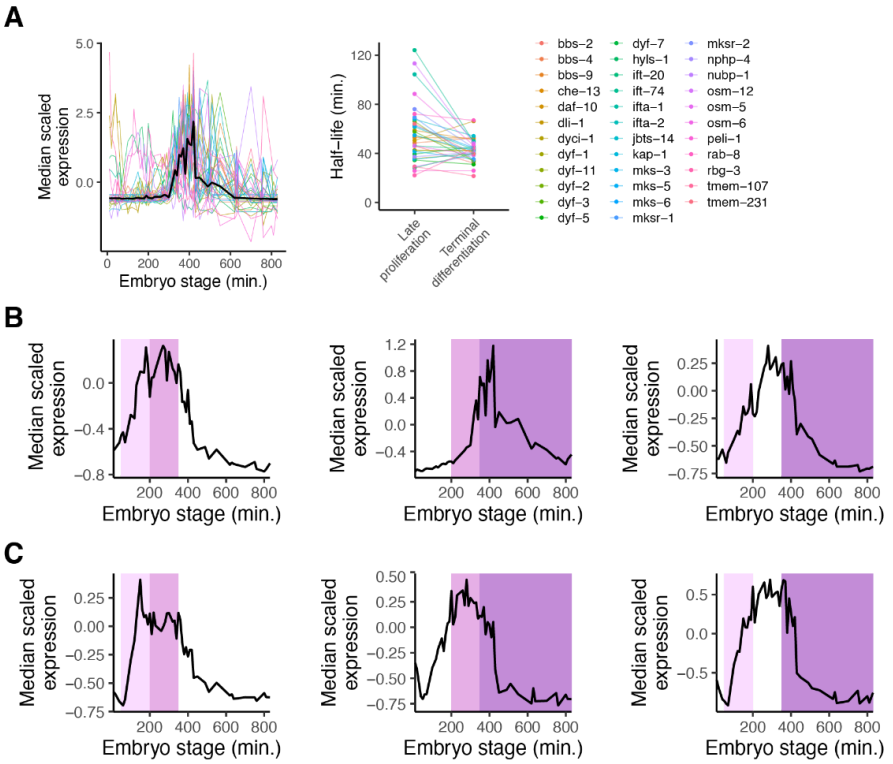

Supplemental Figure S8. Extended analyses for genes with differential mRNA decay over time. (A) *Left*. Median scaled expression of core cilia component genes using data from a whole-embryo RNA-sequencing time series (Hashimshony et al. 2015). *Right*. Plot displaying the change in mRNA half-lives from Middle to Late stage for core cilia component genes. (B) Median scaled expression of zygotic-only genes in the top 5% of genes with faster mRNA decay in a later stage compared to in an earlier stage. Pink shading spans the Early stage, light purple shading spans the Middle stage, and dark purple shading spans the Late stage. (C) Median scaled expression of zygotic-only genes in the top 5% of genes with slower mRNA decay in a later stage compared to in an earlier stage. Pink shading spans the Early stage, light purple shading spans the Middle stage, and dark purple shading spans the Late stage.

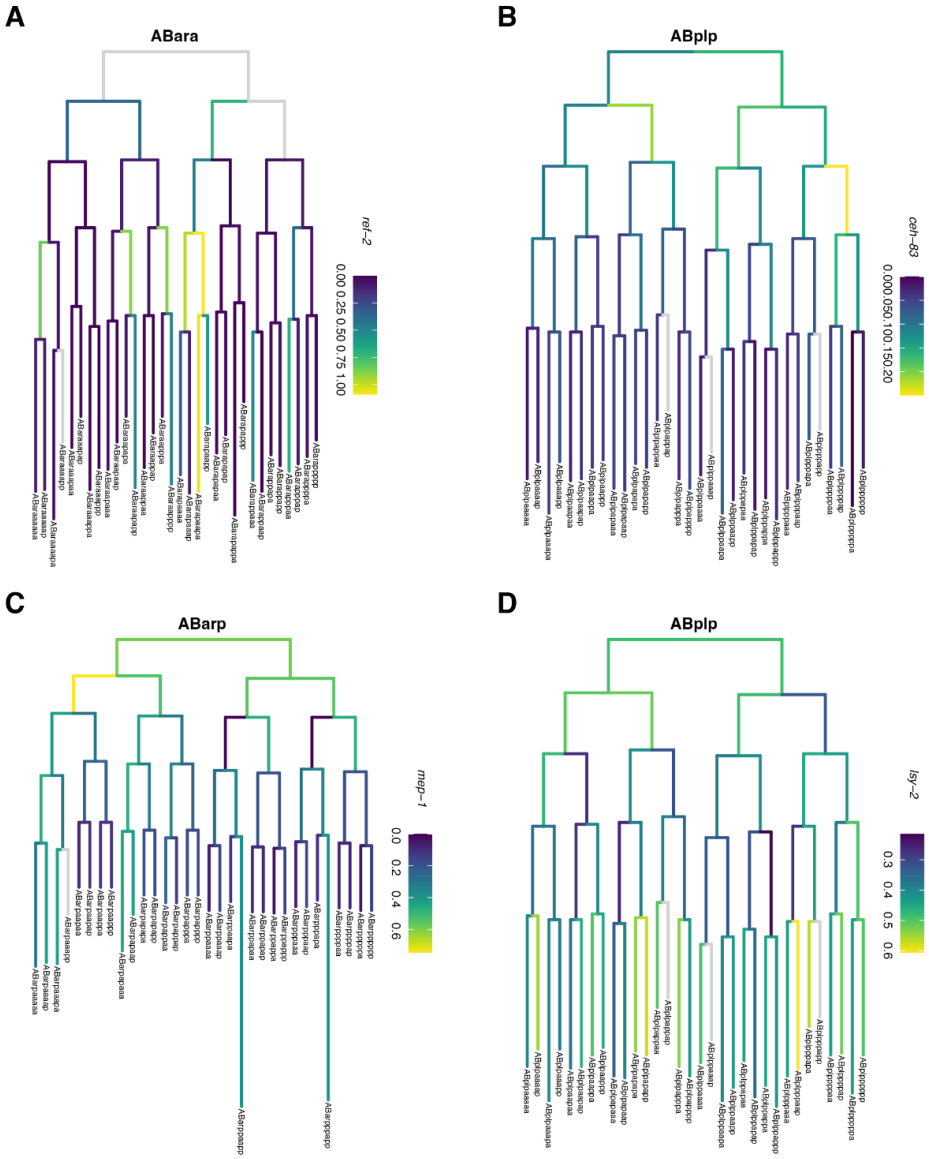

Supplemental Figure S9. Lineage tree examples of transcription factor genes with transient or persistent mRNA expression. (A) Lineage tree for the ABara sublineage with coloring representing *ref-2* mRNA expression from our *C. elegans* embryo single cell atlas (Packer et al. 2019). (B) Lineage tree for the ABplp sublineage with coloring representing *ceh-83* mRNA expression from our *C. elegans* embryo single cell atlas (Packer et al. 2019). (C) Lineage tree for the ABarp sublineage with coloring representing *mep-1* mRNA expression from our *C. elegans* embryo single cell atlas (Packer et al. 2019). (D) Lineage tree for the ABplp sublineage with coloring representing *lsy-2* mRNA expression from our *C. elegans* embryo single cell atlas (Packer et al. 2019).

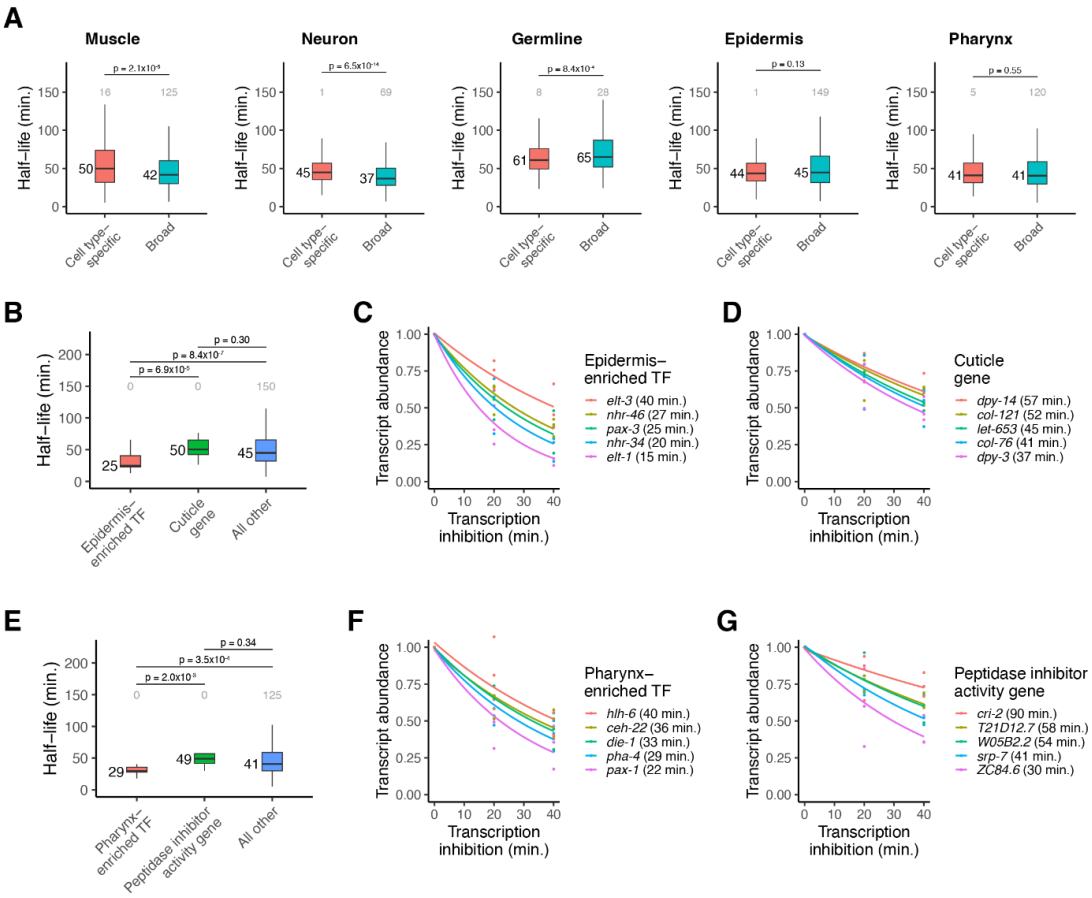

Supplemental Figure S10. mRNA half-lives of cell type-specific genes. (A) Box plots showing the mRNA half-life distributions of cell type-specific and broadly expressed genes within muscle, germline, epidermis, neuron, and pharynx cells. (B) Box plots showing the epidermis-specific mRNA half-life distributions of epidermis-enriched transcription factor genes, cuticle genes, and all other genes. (C) Scatter plot of the normalized transcript abundance of the epidermis-enriched transcription factor genes *elt-3*, *nhr-46*, *pax-3*, *nhr-34*, *elt-1* throughout a 40 minute transcription inhibition time course in epidermal cells. Each point represents normalized transcript abundance from one of three biological replicates. (D) Scatter plot of the normalized transcript abundance of the cuticle genes *dpy-14*, *col-121*, *let-653*, *col-76*, *dpy-3* throughout a 40 minute transcription inhibition time course in epidermal cells. Each point represents normalized transcript abundance from one of three biological replicates. (E) Box plots showing the pharynx-specific mRNA half-life distributions of pharynx-enriched transcription factor genes, peptidase inhibitor activity genes, and all other genes. (F) Scatter plot of the normalized transcript abundance of the pharynx-enriched transcription factor genes *hlh-6*, *ceh-22*, *die-1*, *pha-4, pax-1* throughout a 40 minute transcription inhibition time course in pharynx cells. Each point represents normalized transcript abundance from one of three biological replicates. (G) Scatter plot of the normalized transcript abundance of the peptidase inhibitor activity genes *cri-2*, *T21D12.7*, *W05B2.2*, *srp-7*, *ZC84.6* throughout a 40 minute transcription inhibition time course in pharynx cells. Each point represents normalized transcript abundance from one of three biological replicates. Numbers to the left of the box plots are median half-lives within each group. Numbers above box plots are the number of genes with half-lives greater than 150 minutes within each group. P-values comparing median half-lives were calculated using the Wilcoxon rank sum test.

A

Term	Expected	Observed	Enrichment.Fold.Change	P.value	Q.value
supramolecular polymer GO:0099081	9.9	50	5.1	3.8e–23	5.4e–21
striated muscle dense body GO:0055120	4.5	33	7.4	3.7e–22	3.5e–20
myofibril GO:0030016	3.6	29	8.1	2.8e–21	2.0e–19
extracellular region GO:0005576	3.6	25	7.0	1.1e–16	6.4e–15
A band GO:0031672	1.7	17	10.0	6.0e–16	2.8e–14
muscle system process GO:0003012	1.7	17	9.9	1.5e–15	6.0e–14
sarcomere organization GO:0045214	1.5	16	10.0	2.6e–15	9.1e–14
gated channel activity GO:0022836	2.3	18	8.0	5.6e–14	1.8e–12
passive transmembrane transporter activity GO:0022803	4.2	24	5.7	1.4e–13	3.9e–12
muscle cell development GO:0055001	2.1	17	7.9	2.6e–13	6.7e–12

B

Term	Expected	Observed	Enrichment.Fold.Change	P.value	Q.value
cell projection organization GO:0030030	14.0	78	5.4	4.7e–38	3.4e–36
cilium organization GO:0044782	3.8	41	11.0	4.8e–38	3.4e–36
cell projection GO:0042995	18.0	86	4.8	9.8e–37	4.7e–35
ciliary basal body GO:0036064	2.0	25	13.0	1.3e–27	5.3e–26
non–motile cilium assembly GO:1905515	1.7	21	12.0	3.9e–23	1.4e–21
ciliary plasm GO:0097014	1.1	15	14.0	2.2e–19	6.8e–18
taxis GO:0042330	8.1	37	4.6	2.2e–16	6.1e–15
neuron development GO:0048666	8.8	37	4.2	5.8e–15	1.5e–13
microtubule–based transport GO:0099111	2.6	19	7.3	4.6e–14	1.1e–12
extracellular region GO:0005576	3.2	17	5.3	6.6e–10	1.4e–08

C

Term	Expected	Observed	Enrichment.Fold.Change	P.value	Q.value
extracellular region GO:0005576	3.70	24	6.6	1.5e–15	8.4e–14
molting cycle GO:0042303	2.50	19	7.7	1.9e–14	8.8e–13
organic acid metabolic process GO:0006082	9.40	37	3.9	6.0e–14	2.4e–12
structural constituent of cuticle GO:0042302	0.72	9	13.0	1.4e–11	5.0e–10
oxidoreductase activity acting on CH–OH group of donors GO:0016614	1.90	11	5.8	1.0e–07	3.3e–06
DNA–binding transcription factor activity GO:0003700	9.30	27	2.9	1.4e–07	4.1e–06
microbody GO:0042579	1.60	10	6.1	1.7e–07	4.3e–06
zinc ion binding GO:0008270	7.90	24	3.0	2.3e–07	5.3e–06
iron ion binding GO:0005506	1.20	8	6.5	1.1e–06	2.3e–05
peptidase inhibitor activity GO:0030414	0.59	5	8.5	5.4e–06	1.1e–04

D

Term	Expected	Observed	Enrichment.Fold.Change	P.value	Q.value
serine–type endopeptidase inhibitor activity GO:0004867	0.18	7	40.0	5.4e–14	7.7e–12
peptidase inhibitor activity GO:0030414	0.26	7	26.0	2.5e–11	2.4e–09
endopeptidase regulator activity GO:0061135	0.29	7	24.0	6.3e–11	4.5e–09
DNA–binding transcription factor activity GO:0003700	4.10	19	4.6	6.6e–09	3.8e–07
transcription regulatory region nucleic acid binding GO:0001067	3.80	17	4.5	5.7e–08	2.7e–06
sequence–specific DNA binding GO:0043565	5.20	19	3.7	3.1e–07	1.2e–05
double–stranded DNA binding GO:0003690	4.40	17	3.9	5.6e–07	2.0e–05
pharynx development GO:0060465	0.53	6	11.0	6.2e–07	2.0e–05
cell surface GO:0009986	0.46	5	11.0	4.6e–06	1.3e–04
external encapsulating structure GO:0030312	0.46	4	8.6	7.8e–05	2.0e–03

E

Term	Expected	Observed	Enrichment.Fold.Change	P.value	Q.value
mRNA 3'–UTR binding GO:0003730	4.3	8	1.8	0.0014	0.014
membrane–enclosed lumen GO:0031974	73.0	90	1.2	0.0019	0.018
single–stranded DNA binding GO:0003697	3.4	6	1.8	0.0061	0.056
recombinational repair GO:0000725	3.4	6	1.8	0.0061	0.056
cell part morphogenesis GO:0032990	3.4	6	1.8	0.0061	0.056
neuron development GO:0048666	2.9	5	1.7	0.0130	0.110
identical protein binding GO:0042802	9.7	14	1.4	0.0140	0.110
import into nucleus GO:0051170	5.3	8	1.5	0.0250	0.200
ATP–dependent activity acting on RNA GO:0008186	5.3	8	1.5	0.0250	0.200
extracellular region GO:0005576	2.4	4	1.7	0.0260	0.200

Supplemental Figure S11. Gene ontology analysis of cell type-specific genes. (A) Ten most significantly enriched gene ontology terms for muscle-specific genes that met our moderate mRNA half-life filtering metric within muscle cells. Background set of genes used was all genes that met our moderate mRNA half-life filtering metric within muscle cells. (B) Ten most significantly enriched gene ontology terms for neuron-specific genes that met our moderate mRNA half-life filtering metric within neuronal cells. Background set of genes used was all genes that met our moderate mRNA half-life filtering metric within neuron cells. (C) Ten most significantly enriched gene ontology terms for epidermis-specific genes that met our moderate mRNA half-life filtering metric within epidermal cells. Background set of genes used was all genes that met our moderate mRNA half-life filtering metric within epidermal cells. (D) Ten most significantly enriched gene ontology terms for pharynx-specific genes that met our moderate mRNA half-life filtering metric within pharynx cells. Background set of genes used was all genes that met our moderate mRNA half-life filtering metric within pharynx cells. (E) Ten most

significantly enriched gene ontology terms for germline-specific genes that met our moderate mRNA half-life filtering metric within germline cells. Background set of genes used was all genes that met our moderate mRNA half-life filtering metric within germline cells.